Bioelectrochemistry 90 (2013) 18–23

Contents lists available at SciVerse ScienceDirect

Bioelectrochemistry

journal homepage: www.elsevier.com/locate/bioelechem

Amperometric immunobiosensor for α-fetoprotein using Au nanoparticles/chitosan/TiO_2–graphene composite based platform

Ke-Jing Huang *, Jing Li, Ying-Ying Wu, Yan-Ming Liu *

College of Chemistry and Chemical Engineering, Xinyang Normal University, Xinyang 464000, P.R. China

ARTICLE INFO

Article history:
Received 24 September 2011
Received in revised form 7 October 2012
Accepted 8 October 2012
Available online 7 November 2012

Keywords:
TiO_2–graphene nanocomposite
Gold nanoparticles
Lable-free
α-fetoprotein
Immunosensor

ABSTRACT

A simple label-free amperometric immunosensor for protein detection is developed based on TiO_2–graphene (TiO_2–Gr), chitosan and gold nanoparticles (AuNPs) composite film modified glassy carbon electrode (GCE). The negatively charged AuNPs can be adsorbed on the positively charged chitosan/TiO_2–Gr composite film by electrostatic adsorption, and then is used to immobilize α-fetoprotein antibody for the assay of α-fetoprotein (AFP). The interaction of antigen and antibody on the electrode interface makes a barrier for electrons and inhibits the electro-transfer, resulting in the decreased DPV signals of probe $Fe(CN)_6^{3-/4-}$. Using this strategy, a wide detection range (0.1–300 ng mL^{-1}) with the correlation coefficients of 0.992–0.994 for model target AFP is obtained. The limit of detection is 0.03 ng mL^{-1} at a signal-to-noise ratio of 3. The results prove that the sensing strategy possesses sensitivity, selectivity, stability and generality, and it may be used to immobilize other biomoleculars to develop biosensor for the detection of other antigens or biocompounds.

1. Introduction

Cancer biomarkers are molecules occurring in blood or tissue, which are associated with cancer and whose measurement or identification play an important role in patient diagnosis and clinical research [1,2]. α-Fetoprotein (AFP) is an oncofetal glycoprotein with a molecule weight of approximately 70 kDa. It is one of the most extensively used clinical cancer biomarkers [3]. The average concentration of AFP in healthy human serum is about 25 ng mL^{-1} [4]. Elevated AFP concentration in serum may be an early indication of some cancerous diseases such as hepatocellular cancer, liver metastasis from gastric cancer, testicular cancer, and nasopharyngeal cancer [5]. Thus, the detection of AFP is absolutely necessary in clinical assay.

Recently, immunoassays have gained increasing attention in the quantitative detection of AFP because of their high selectivity, such as surface plasmon resonance [6], fluorescence measurement [7], mass spectrometry [8], chemiluminescence assay [9], micellar electrokinetic capillary chromatography [10] and electrochemical assay [11]. Among these methods, electrochemical immunosensor has been a promising alternative to conventional immunoassay due to its cost efficiency, excellent sensitivity and inexpensive instrumentation [12,13]. One key research area of electrochemical immunosensors is development of biosensors with various materials with nanoparticle-like physical and chemical properties because they can provide a large surface area and improve the biocompatibility and stability of the biosensors [14,15].

Graphene (Gr)-based nanocomposites have attracted considerable attention due to their remarkable electrocatalytic, electrochemical sensing and electrochemical energy conversion properties [16–18]. They exhibit unique structure of one-atom-thick and two-dimensional layers of sp^2-bonded carbon, which has high surface areas (theoretical value of 2630 $m^2\ g^{-1}$) and mobility of charge carriers (200,000 $cm^2\ V^{-1}\ s^{-1}$). These properties make Gr an ideal two-dimensional catalyst support to anchor metal and semiconductor catalyst nanoparticles, offering versatile selective catalytic or sensing performances [19,20]. The Gr-based nanocomposite hybrid materials have shown greater versatility as advanced electrode materials for the fabrication of electrochemical sensors and biosensors [21,22]. Due to its good biocompatibility and high conductivity, TiO_2 has been widely used in the fabrication of electrochemical biosensors [23–26]. In these biosensors, TiO_2 was employed as support matrix for immobilizing enzymes. The results showed that the TiO_2-based composites can facilitate the direct electron transfer and enhance the catalytic activity of enzymes. Most recently, we reported the TiO_2–graphene (TiO_2–Gr) nanocomposite prepared by hydrothermal method using Gr as template to immobilized TiO_2 nanoparticles [27]. The as-prepared TiO_2–Gr exhibited remarkable electrocatalytic activity towards dopamine oxidation. Using this TiO_2–Gr biosensor, excellent analytical performance, such as high selectivity, broad dynamic range and low detection limit, has been achieved for the determination of dopamine. These characteristics and advantages of TiO_2–Gr nanocomposites opened a new platform for electrochemical sensors and biosensors design.

Gold nanoparticles (AuNPs) are well-known bio-nanomaterials because of their large specific surface area, strong adsorption ability, well suitability and good conductivity [28,29]; it can strongly interact

* Corresponding author. Tel.: +86 376 6390611.
E-mail addresses: kejinghuang@163.com (K.-J. Huang), liuym9518@sina.com (Y.-M. Liu).

1567-5394/$ – see front matter © 2012 Elsevier B.V. All rights reserved.
http://dx.doi.org/10.1016/j.bioelechem.2012.10.005

with biomaterials and has been utilized as an intermediator to immobilize antibody to efficiently retain its activity and to enhance current response in the construction of immunosensor. Chitosan (Chit) is a polysaccharide derived by deacetylation of chitin. It possesses many advantages such as excellent membrane-forming ability, high permeability towards water, good adhesion and biocompatibility. Also, it has abundant reactive amino and hydroxyl functional groups. So it has been widely used as an immobilization matrix for biofabrication. Herein, Chit is used in the immunosensor preparation. It makes the Chit–TiO_2–Gr composite film more uniform and it also can adsorb AuNPs to the electrode surface by electrostatic interaction.

In this work, an electrochemical immunosensor was designed based on TiO_2–Gr, Chit and AuNPs composite modified glassy carbon electrode (GCE). The preparation, characterization, optimal conditions, and preliminary analysis of real samples for the detection of AFP were investigated. It showed that AuNPs/Chit/TiO_2–Gr nanocomposite film could effectively facilitate the direct electron transfer of probe $Fe(CN)_6^{3-/4-}$ to the electrode, and thus greatly improve the sensitivity of the immunosensor. This developed biosensor showed good performances, such as high sensitivity, good stability and good selectivity, and wide linear range owing to the synergistic effects of TiO_2–Gr, Chit and AuNPs. This strategy can be further developed for practical clinical detection of AFP and other important tumor markers.

2. Experimental

2.1. Materials

Chloroauric acid, sodium citrate, iron chloride hexahydrate, potassium ferricyanide, graphite powder, hydrazine solution (50 wt.%) and ammonia solution (28 wt.%) was obtained from Shanghai Chemical Reagent Corporation (Shanghai, China). Bovine serum albumin (BSA), carcinoembryonic antigen (CEA), low density lipoprotein (LDL), prostate-specific antigen (PSA) and human immunoglobulin (HIgG) were obtained from Sigma (Saint Louis, MO, USA). AFP, alpha-fetoprotein antibody (anti-AFP, polyclonal), and AFP ELISA kits were purchased from Biocell (Zhengzhou, China). Phosphate-buffered saline (PBS, 0.01 M) at various pH values was prepared by mixing a stock standard solution of KH_2PO_4 and K_2HPO_4, which was used as the measuring buffer, and then adjusting the pH with 0.1 M KOH and H_3PO_4. Gold nanoparticles were produced by reducing gold chloride tetrahydrate with citric acid at 100 °C for half an hour [30]. The mean size of the prepared Au colloids was about 20 nm. A 0.50 wt.% chitosan stock solution was prepared by dissolving chitosan flakes in hot (80–90 °C) water with 0.05 M HCl. After the solution was cooled to room temperature, the pH was adjusted to 3.5–5.0 with NaOH solution. Chitosan solution was filtered using a 0.45 μm Millex-HA syringe filter unit (Millipore) and stored at 4 °C when not in use. Serum samples provided by Xinyang Central Hospital (Xinyang, China) were stored at 4 °C. All other chemicals were of analytical grade and used without further purification. Ultrapure water (18.2 MΩ) was obtained from a Milli-Q water purification system and used throughout.

2.2. Instruments

CHI660D electrochemical workstation (CH Instruments, Shanghai, China) and a standard three-electrode cell containing a platinum wire auxiliary electrode, a saturated calomel reference electrode (SCE) and the modified electrode as working electrode were employed for electrochemical studies. All of the potentials in this article were with respect to SCE. The pH measurements were made with a pH meter (MP 230, Mettler–Toledo, Greiffensee, Switzerland).

2.3. Preparation of TiO_2–GR nanocomposite

Graphene oxide (GO) was prepared from graphite powder by the modified Hummers method [31,32]. Graphite was put into a mixture of 12 mL concentrated H_2SO_4, 2.5 g $K_2S_2O_8$ and 2.5 g P_2O_5. The solution was heated to 80 °C and kept stirring for 5 h using oil-bath. Next, the mixture was diluted with deionized water (500 mL). The product was obtained by filtering using 0.2 μm Nylon film and dried naturally. The product was re-oxidized by Hummers and Offeman method to produce the graphite oxide. Exfoliation was carried out by sonicating 0.1 mg mL^{-1} graphite oxide dispersion for 1 h. TiO_2–Gr nanocomposite was prepared according to the previously work [27]. In short, 20 mg of GO was dispersed in a mixed solution of H_2O (10 mL) and ethanol (5 mL) under ultrasonication for 1 h to get a homogenous colloidal suspension of exfoliated GO. Then, 0.2 mL of $Ti(O^iPr)_4$ was added to the GO suspension and ultrasonicated for another 1 h. The resultant mixture was transferred to a 25-mL Teflon-sealed autoclave and kept at 130 °C for 12 h. The final product was isolated by filtration and rinsed thoroughly with water and ethanol, respectively. Then the product was dried in vacuum. The TiO_2–Gr nanocomposite was obtained in the form of black powder.

2.4. Fabrication of the immunosensor

1.0 mg of the as-prepared TiO_2–Gr nanocomposite was dispersed into 1.0-mL Chit solution (1 mg mL^{-1}). The mixture was sonicated for 3 h to obtain a homogeneous suspension. The suspension was sonicated for 15 min immediately before preparing the Chit–TiO_2–Gr films.

Prior to the modification, the bare GCE (3 mm diameter) was carefully polished to obtain a mirror-like surface with 1.0, 0.3 and 0.05 μm alumina aqueous slurry chamois leather, and then was subjected to ultrasonic vibration in absolute ethanol to remove residual alumina particles and rinsed with doubly distilled water followed by ethanol.

After carefully washed with water, the GCE was treated by dropping 6 μL of Chit–TiO_2–Gr suspension and then dried in air. The prepared Chit–TiO_2–Gr/GCE was immersed in AuNPs solution and left for 10 h to adsorb a layer of AuNPs on GCE surface. After rinsed with water, the resultant electrode was immersed in anti-AFP solution and was kept at 4 °C for 12 h for immobilization of anti-AFP. The antibody-modified electrode was then thoroughly washed with PBS and subsequently was incubated in BSA solution (w/w, 0.25%) for 2 h in order to block possible remaining active sites and avoid the non-specific adsorption. After washed carefully with PBS, the immunosensor was fabricated and stored at 4 °C when not in use. The preparation process of immunosensor was shown in Scheme 1.

2.5. Electrochemical measurements

The electrochemical characteristics of the modified electrode were characterized by cyclic voltammetry (CV). Electrochemical measurements were done in a conventional electrochemical cell. CV scans were taken in 5-mL PBS with a scan rate of 100 mV s^{-1}. The measurement was based on the changes in amperometric response before and after the antigen–antibody reaction. After incubation in antigen, the peak current response of the immunosensor was expected to decrease, because the antigen–antibody immunocomplex hindered the access of the electron to the electrode. The amount of immunocomplex increased when the concentration of antigen increased, and this resulted in a decrease in the current response.

3. Results and discussion

3.1. Characterizations

The surface morphologies of TiO_2–Gr and AuNPs/TiO_2–Gr–Chit composite were examined by SEM observation (Fig. 1). In Fig. 1A, it

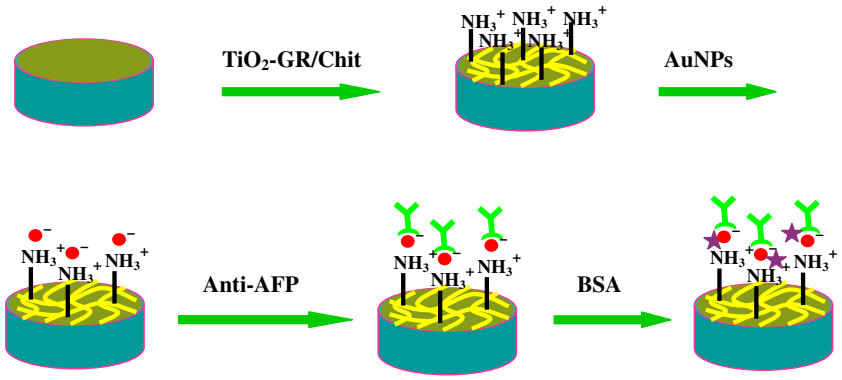

Scheme 1. The stepwise fabrication process of the immunosensor.

can be seen that TiO2 was formed in a highly faceted morphology on the substrates of Gr. Fig. 1B presented the SEM image of AuNPs/TiO2–Gr–Chit composite. It was shown that AuNPs was formed on the TiO2–Gr–Chit surface.

The CV of ferricyanide was chosen as a marker to investigate the changes of the electrode behavior before and after each assembly step. All electrochemical measurements were performed in PBS (pH 7.0) containing 0.1 M KCl and 5 mM $Fe(CN)_6^{3-/4-}$. Fig. 2(A) showed the CVs of $Fe(CN)_6^{3-/4-}$ at the bare GCE, Chit/GCE, AuNPs–Chit/GCE, TiO_2–Gr–Chit/GCE and AuNPs/TiO_2–Gr–Chit/GCE, respectively. A decreased current respond was observed after Chit was modified on the GCE. In comparison with Chit/GCE and GCE, the peak currents increase after AuNPs modification (curve c). The reason is that AuNPs could act as an electron shuttle, which makes it easier for the electrons transfer to take place [33]. It was observed that the peak current of TiO_2–Gr–Chit/GCE greatly increased compared to that of above electrodes (curve d). Obviously, the TiO_2–Gr film increased the conductivity and stability of TiO_2–Gr–Chit/GCE because TiO_2–Gr nanocomposites could increase surface area and active sites for electron transfer. When the GCE was simultaneously modified with TiO_2–Gr and AuNPs, the current respond greatly increased (curve e). The synergistic effect of TiO_2–Gr and AuNPs significantly improved the electron-transfer efficiency of the modified electrode.

As shown in Fig. 2(B), a decreased current response was observed on anti-AFP/AuNPs/TiO_2–Ge–Chit/GCE (curve b) compared to that on AuNPs/TiO_2–Ge–Chit/GCE (curve a), because the immobilized anti-AFP acted as insulator blocking the electron transfer. This also indicated that anti-AFP had been immobilized on the electrode surface. Subsequently, the immunosensor was blocked with BSA solution and then incubated in an incubation solution containing AFP. It could be found that the peak currents of the curves c and d were decreased comparing with curve b. This may originate from the insulating BSA and AFP protein

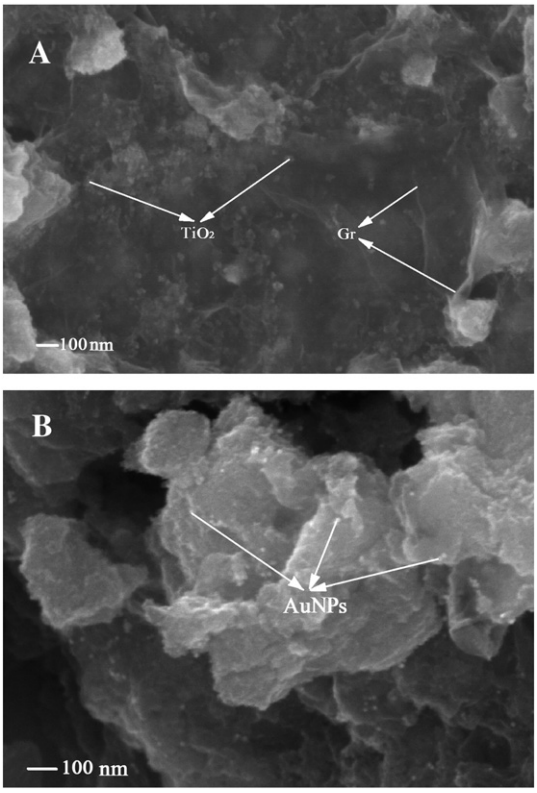

Fig. 1. SEM images of TiO_2–Gr (A) and AuNPs/TiO_2–Gr–Chit nanocomposite (B).

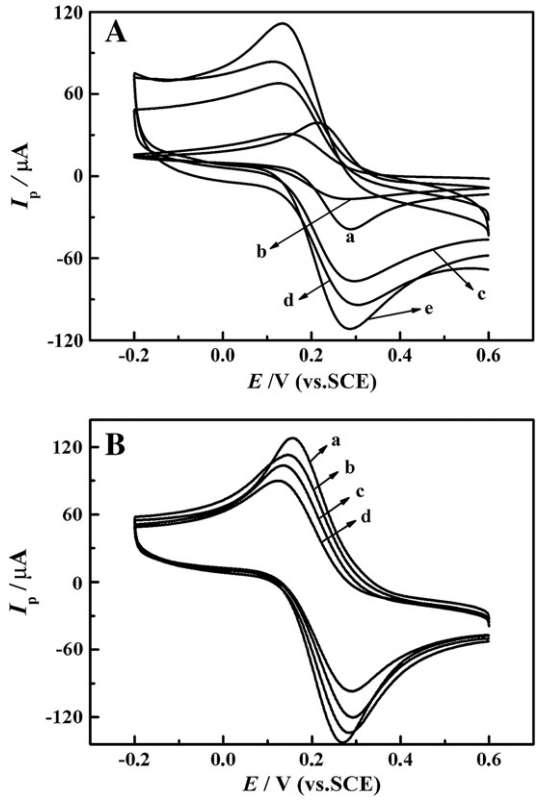

Fig. 2. Cyclic voltammograms of different modified electrodes in pH 7.0 PBS containing 0.1 M KCl and 5.0 mM $Fe(CN)_6^{3-/4-}$. (A): a, bare GCE; b, Chit/GCE; c, AuNPs–Chit/GCE; d, TiO_2–Gr–Chit/GCE; e, AuNPs/TiO_2–Gr–Chit/GCE. (B): a, AuNPs/TiO_2–Gr–Chit/GCE; b, anti-AFP/AuNPs/TiO_2–Gr–Chit/GCE; c, BSA/anti-AFP/AuNPs/TiO_2–Gr–Chit/GCE; d, AFP/BSA/anti-AFP/AuNPs/TiO_2–Gr–Chit/GCE. C(AFP) = 150 ng mL^{-1}. Scan rate: 100 mVs^{-1}.

layers, which can hinder the transmission of electrons toward the electrode surface.

Typical CV curves of the proposed anti-AFP/AuNPs/TiO_2–Gr–Chit/GCE in 0.1 M PBS at different scan rates were shown in Fig. 3. It could be seen that a pair of roughly symmetric anodic and cathodic peaks appeared with almost equal peak currents in the scan rate range from 0.01 to 0.250 Vs^{-1}. The peak-to-peak separation also increased with the scan rate. According to Randles–Sevcik equation,

$$I_p = 0.4463\left(F^3/RT\right)^{1/2} n^{3/2} A_0 {D_0}^{1/2} C_0 A v^{1/2} \quad (1)$$

where A_0 is the electrode area (cm^2), D_0 is the diffusion coefficient ($cm\ s^{-1}$), C_0 is the concentration of the electro-active species ($mol\ L^{-1}$), ν is the scan rate, and n, I_p, F, R, and T have their usual meanings, good linear relationship was found for the peak current and the square root of scan rate, with the results shown in Fig. 3 (upper right inset). The reduction and oxidation peak currents rose linearly with the linear egression equations as I_{pa} (μA) = $(1.791 \pm 0.021)\nu^{1/2}$ ($mV\ s^{-1}$)$^{1/2}$ + (12.855 ± 0.091) ($R = 0.997$) and I_{pc} (μA) = $(-1.915 \pm 0.031)\nu^{1/2}$ ($mV\ s^{-1}$)$^{1/2}$ − (8.296 ± 0.018) ($R = 0.995$), respectively, suggesting a diffusion-confined redox process.

3.2. Optimization of experimental parameters

The pH of the measuring solution may affect the immunosensor response signals. Unsuitable pH not only cause protein denaturalization, but affected the affinity between the protein and the electrode surface. The effect of pH on the immunosensor was evaluated in the range of 4.0–8.0. As shown in Fig. 4, the current response reached the maximum at pH 7.0, and then decreased when the pH was higher or lower than this value. The higher or lower pH may damage the protein and affected the lifetime of the immunosensor. So, the pH 7.0 was used for further experiments.

Temperature is important on the activity of the antigen and antibody. The effect of temperature was studied in the range of 20–45 °C. The results showed that the peak current gradually decreased as temperature increased from 20 to 35 °C, and then increased as temperature increased above 35 °C. This may be attributed to the fact that more and more immunocomplex formed and inhibited the current response

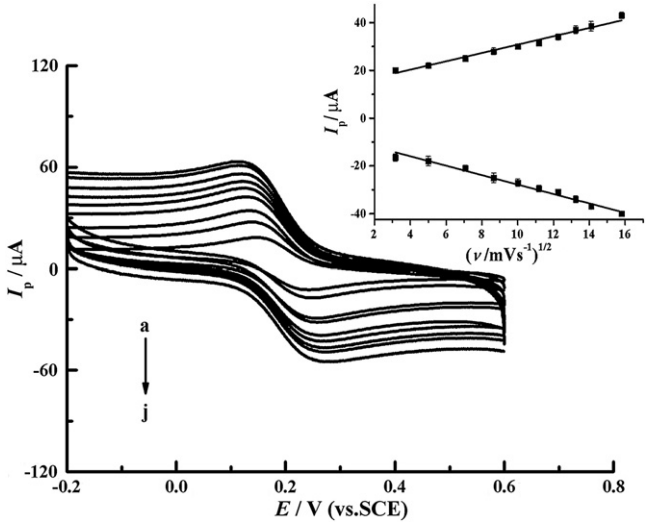

Fig. 3. CVs of the anti-AFP/AuNPs/TiO_2–Gr–Chit/GCE in pH 7.0 PBS containing 0.1 M KCl and 5.0 mM $Fe(CN)_6^{3-/4-}$ at the different scan rate of (from a to j): 10, 25, 50, 75, 100, 125, 150, 175, 200, 250 mVs^{-1}. The inset shows the linear relationship between the peak currents and the square root of scan rate. C(AFP) = 250 ng mL^{-1}. Regression equation: I_{pa} (μA) = $(1.791 \pm 0.021)\nu^{1/2}$ ($mV\ s^{-1}$)$^{1/2}$ + (12.855 ± 0.091); I_{pc} (μA) = $(-1.915 \pm 0.031)\nu^{1/2}$ ($mV\ s^{-1}$)$^{1/2}$ − (8.296 ± 0.018).

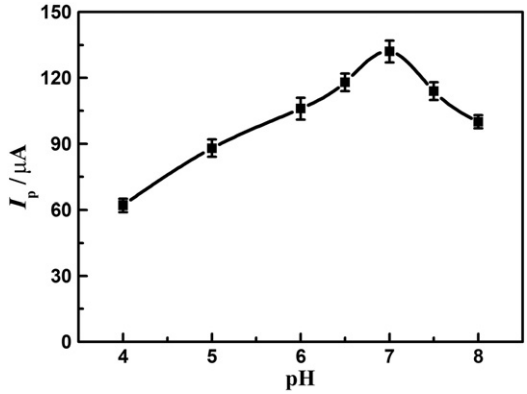

Fig. 4. Effects of pH of PBS in the presence of 30 ng mL^{-1} of AFP on the response signals.

during the temperature increase from 20 to 35 °C. However, temperature above 40 °C might cause irreversible denaturation of AFP and anti-AFP. As is well known, 37 °C could be an optimal temperature of immunoreaction; however, long-time use in high temperature may damage the modifier and affect the lifetime of the immunosensor. Taking into account the activity, lifetime, and response characteristics of biomolecules, room temperature (25 ± 2 °C) was recommended as the optimal incubation temperature for practical application.

The incubation time was another influence condition of the immunosensor. When antigens reached the antibodies that were modified on the surface of the immunosensor, it would take some time for the contracting species to form immunocomplexes. The effect of incubation time on the response signals was investigated in the range of 2–30 min. With incubation time increased, the peak current rapidly decreased. The current respond reached a steady state after 20 min, indicating the antigen molecules in the solution were almost completely captured by the immobilized antibody molecules. Therefore, 20 min of incubation time was used in the subsequent work.

3.3. Analytical performance of immunosensor

The electrochemical detection of AFP was based on the variation of current response before and after immunoreaction. As expected, the current response signal decreased with increase of AFP concentration. It could be understood that more AFP could bind to the immobilized antibodies at higher concentrations of antigens, and the antigen–antibody complex acted as an inert kinetic barrier for the electron-transfer of the mediator of ferricyanide. As a result, the amperometric response decreased. Fig. 5 showed that the peak currents of the sensor decreased

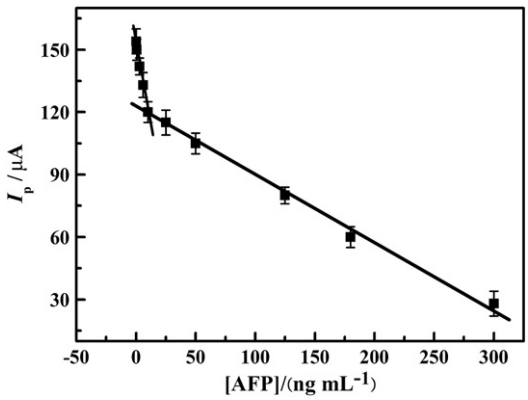

Fig. 5. Calibration curve of the immunosensor for AFP determination. The amperometric measurement was carried out by CVs in 0.1 M PBS (pH 7.0). Regression equation: I (μA) = (-3.298 ± 0.042) C ($ng\ mL^{-1}$) + (152.73 ± 5.23) (0.1–10.0 ng mL^{-1}); I (μA) = (-0.321 ± 0.004) C ($ng\ mL^{-1}$) + (121.63 ± 3.42) (10.0–300.0 ng mL^{-1}). Scan rate: 100 mVs^{-1}.

Table 1
Comparison of different electrochemical immunosensors for the determination of AFP.

Modified electrode	Linear range (ng mL^{-1})	Detection limit (ng mL^{-1})	Reference
anti-AFP/AuNPs/Thi/DNA/MWCNTs-PDDA/AuNPs/GCE	0.1–10 and 10–200	0.04	[35]
Ab-HRP/AFP/anti-AFP/PA/AuNPs/GCE	5–80	3.7	[36]
anti-AFP/AuNPs/Thi/Nafion-MWCNT/GCE	0.8–20 and 20–200	0.26	[37]
anti-AFP/SV-AuNPs/GCE	1.25–200	0.23	[38]
anti-AFP/AuNPs/CNTs/Chit/GCE	1–55	0.6	[34]
anti-AFP/AuNPs/PB/AuNPs/ITO	0.25–300	0.04	[39]
anti-AFP/AuNPs/Thi/Chit–GNPs/GCE	0.4–200	0.24	[40]
anti-AFP/AuNPs/TiO_2–Gr–Chit/GCE	0.1–10 and 10–300	0.03	This work

with an increase of AFP concentration in two ranges: (i) from 0.1 to 10.0 ng mL^{-1} with a regression equation of I (μA) = (−3.298 ± 0.042) C (ng mL^{-1}) + (152.73 ± 5.23) and a correlation coefficient of 0.992, and (ii) from 10.0 to 300.0 ng mL^{-1} with a regression equation of I (μA) = (−0.321 ± 0.004)C (ng mL^{-1}) + (121.63 ± 3.42) and correlation coefficient of 0.994. The detection limit was 0.03 ng mL^{-1} (S/N = 3). Why do the calibration curves present two linear segments? The reason may be: the amount of antibody immobilized on the immunosensor is limited. Antigen binds with the active sites of antibody which is immobilized on the immunosensor when the immunosensor is used to detect antigen. With increase of antigen concentration, active sites of antibody on the immunosensor become fewer and fewer. As a result, the sensitivity declines when the immunosensor is used to determine higher concentration of antigen. The analytical performance of the proposed immunoassay has been compared with those of other AFP immunoassays reported (Table 1). The comparative data suggested superiority of the present sensor over some earlier reported methods, especially the detection limit.

3.4. Precision, selectivity, stability and regeneration

The precision of the immunosensors was investigated by using the variation coefficients (CVs) of intra- and inter-assays. The intra-assay precision of the analytical method was evaluated by analyzing 5 concentration levels of analyte for five times per run. The CVs of intra-assay were 4.2%, 4.0%, 3.9%, 4.9% and 4.8% at 0.1, 1, 10, 100, and 300 ng mL^{-1} of AFP, respectively. Similarly, the CVs of the inter-assay were 5.8%, 6.4%, 5.2%, 6.9%, and 5.6% at 0.1, 1, 10, 100, and 300 ng mL^{-1} of AFP, respectively. Thus, the precision and reproducibility of the immunosensors was acceptable.

Selectivity is one of the potential advantages of using biological molecules as recognition elements in immunosensors. To monitor the differences in response of the immunosensor to interference degree or crossing recognition level, some proteins including 200 ng mL^{-1} CEA, 200 ng mL^{-1} LDL, 200 ng mL^{-1} PSA, 200 ng mL^{-1} HIgG and 200 ng mL^{-1} BSA were used to evaluate the selectivity of the immunosensors, respectively. The immunosensors were separately exposed to two types of 100 ng mL^{-1} AFP incubating solution: one with interference and the other without. The results were shown in Table 2, which indicated that the selectivity of the as-prepared immunosensor was acceptable within experimental error.

Table 2
Interference studies with the immunosensor.

Interferent	CEA	LDL	PSA	HIgG	BSA
Current (μA)[a]	94.56	92.87	95.72	96.23	92.20
Current (μA)[b]	94.90	93.54	94.50	95.12	93.50
Difference of current ratio[c] (%)	0.35	0.72	−1.27	−1.15	1.41

[a] Anodal peak current responses after immunosensors incubated with 100 ng mL^{-1} AFP without the interference.
[b] Anodal peak current responses after immunosensors incubated with 100 ng mL^{-1} AFP with the interference.
[c] Difference of current ratio = $(I_b - I_a)/I_a$.

The stability of the developed immunosensor was examined. When the proposed immunosensor was stored at 4 °C and measured every 5 days, the peak current of the conserved immunosensor increased only 3.48% and 5.16% of its initial response after storing for 20 and 30 days, respectively. Obviously, the resulting immunosensor achieved sufficient stability. This indicated TiO_2–GR/Chit had better electrochemical stability and the anti-AFP biomolecules were stably immobilized on the AuNPs monolayer, which provided a good biocompatible microenvironment for biomolecules to retain their bioactivity.

Regeneration is an important characteristic of a practical immunosensor. In this experiment, immunosensor was immersed in 4 mol L^{-1} urea solution for 5 min and then washed with water to dissociate the antigen–antibody complex. A response error of 2.6% was obtained over 5 regeneration and measurement cycles.

3.5. Sample analysis

To monitor the analytical reliability and possible application of the developed immunosensor, recovery experiments were performed by standard addition methods in human serum. Five freeze-drying standard samples were dissolved in the negative (normal) human serum samples at different AFP concentrations and analyzed by using the developed immunosensor. The results were summarized in Table 3. The results showed that the recoveries were in the range of 92.6–108.1%. The relative standard deviations (RSD) were 2.4–4.2%. Furthermore, some serum specimens were divided into two aliquots and evaluated by using the electrochemical immunoassay and the referenced ELISA method, respectively. As shown in Fig. 6, both results were in acceptable agreement. Thus, the developed immunosensor provided a possible application for the detection of AFP in clinical diagnostics.

4. Conclusions

In the present work, a novel strategy of an amperometric immunosensor for AFP was developed based on the antibody adsorbed in AuNPs/Chit/TiO_2–Gr/GCE. The combination of the good conductivity and a large surface area of TiO_2–Gr, and the advantages of the AuNPs, including biocompatibility and amplification, enhanced the sensitivity of the immunosensor significantly. The biosensor possesses good bioactivity, comparable detection limit and linear range, and acceptable storage stability. The results showed that the method was simple and sensitive enough for determination of AFP in real samples with good

Table 3
Recoveries experiment in serum samples with the immunosensor (n = 3).

Samples	Standard value of AFP (ng mL^{-1})	Determined value of AFP (ng mL^{-1})	Recovery (%)	RSD (%)
1	0.3	0.32	106.7	3.4
2	3.0	3.15	105.0	4.2
3	30.0	29.46	98.2	3.6
4	100.0	92.6	92.6	2.4
5	150.0	162.15	108.1	3.8

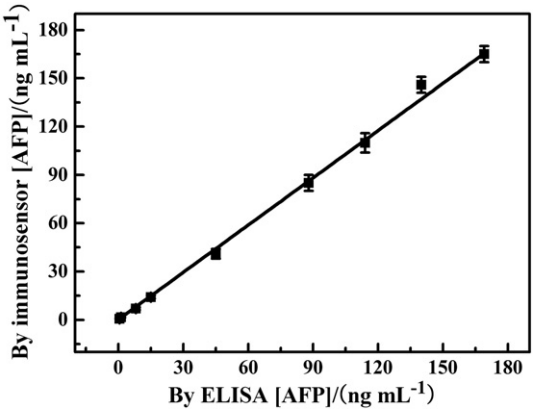

Fig. 6. Correlation between AFP levels measured in real serum samples using the developed immunosensor and ELISA results. Regression equation: *y*(value detected by immunosensor) = (0.978 ± 0.012)x(value detected by ELISA) + (0.201 ± 0.010).

precision and accuracy. Immunosensor fabrication was versatile, and could be easily extended to other biomolecule detection.

Acknowledgments

This work was supported by the National Natural Science Foundation of China (21075106), Program for Science & Technology Innovation Talents in Universities of Henan Province (2010HASTIT025), and Excellent Youth Foundation of He'nan Scientific Committee (104100510020).

References

[1] M. Miyake, K. Sugano, H. Sugino, K. Imai, E. Matsumoto, K. Maeda, S. Fukuzono, Y. Hirao, Fibroblast growth factor receptor 3 mutation in voided urine is a useful diagnostic marker and significant indicator of tumor recurrence in non-muscle invasive bladder cancer, Cancer Sci. 101 (2010) 250–258.
[2] B. Zhang, X. Zhang, H.H. Yan, S.J. Xu, D.H. Tang, W.I. Fu, A novel multi-array immunoassay device for tumor markers based on insert-plug model of piezoelectric immunosensor, Biosens. Bioelectron. 23 (2007) 19–25.
[3] X.W. Wang, H. Xie, Alpha-fetoprotein enhances the proliferation of human hepatoma cells in vitro, Life Sci. 64 (1999) 17–23.
[4] D.P. Tang, R. Yuan, Y.Q. Chai, Direct electrochemical immunoassay based on immobilization of protein-magnetic nanoparticle composites on to magnetic electrode surfaces by sterically enhanced magnetic field force, Biotechnol. Lett. 28 (2006) 559–565.
[5] Y.Y. Xu, C. Bian, S.F. Chen, S.H. Xia, A microelectronic technology based amperometric immunosensor for [alpha]-fetoprotein using mixed self-assembled monolayers and gold nanoparticles, Anal. Chim. Acta 561 (2006) 48–54.
[6] A. Kokado, A. Tsuji, M. Maeda, Chemiluminescence assay of alkaline phosphatase using cortisol-21-phosphate as substrate and its application to enzyme immunoassays, Anal. Chim. Acta 337 (1997) 335–340.
[7] T. Matsuya, S. Tashiro, N. Hoshino, N. Shibata, Y. Nagasaki, K. Kataoka, A core-shell-type fluorescent nanosphere possessing reactive poly(ethylene glycol) tethered chains on the surface for zeptomole detection of protein in time-resolved fluorometric immunoassay, Anal. Chem. 75 (2003) 6124–6132.
[8] S.C. Zhang, C. Zhang, Z. Xing, X.R. Zhang, Simultaneous determination of -detoprotein and free ß-human chorionic gonadotropin by element-tagged immunoassay with detection by inductively coupled plasma mass spectrometry, Clin. Chem. 50 (2004) 1214–1221.
[9] M.D. Xue, T. Haruyama, E. Kobatake, M. Aizawa, Electrochemical luminescence immunosensor for [alpha]-fetoprotein, Sensors Actuators B 36 (1996) 458–462.
[10] R.Y. Wang, X.N. Lu, W.Y. Ma, Non-competitive immunoassay for alpha-fetoprotein using micellar electrokinetic capillary chromatography and laser-induced fluorescence detection, J. Chromatogr. B 779 (2002) 157–162.
[11] L. Zhang, R. Yuan, X. Huang, Y. Chai, S. Cao, Potentiometric immunosensor based on antiserum of Japanese B encephalitis immobilized in nano-Au/polymerized o-phenylenediamine film, Electrochem. Commun. 6 (2004) 1222–1226.
[12] U. Lad, S. Khokhar, G. Kale, Electrochemical creationine biosensors, Anal. Chem. 80 (2008) 7910–7917.
[13] H. Zhang, Q. Zhao, X. Li, X. Le, Ultrasensitive assays for proteins, Analyst 132 (2007) 724–737.
[14] M. Zhou, Y.M. Zhai, S.J. Dong, Electrochemical sensing and biosensing platform based on chemically reduced graphene oxide, Anal. Chem. 81 (2009) 5603–5613.
[15] S.E. Moulton, J.N. Barisci, A. Bath, R. Stella, G.G. Wallace, Investigation of Ig. G adsorption and the effect on electrochemical responses at titanium dioxide electrode, Langmuir 21 (2005) 316–322.
[16] C. Shan, H. Yang, D. Han, Q. Zhang, A. Ivaska, L. Niu, Graphene/AuNPs/chitosan nanocomposites film for glucose biosensing, Biosens. Bioelectron. 25 (2010) 1070–1074.
[17] K.J. Huang, D.J. Niu, X. Liu, Z.W. Wu, Y. Fan, Y.F. Chang, Y.Y. Wu, Direct electrochemistry of catalase at amine-functionalized graphene/gold nanoparticles composite film for hydrogen peroxide sensor, Electrochim. Acta 56 (2011) 2947–2953.
[18] D. Li, R. Kaner, Graphene-based materials, Science 320 (2008) 1170–1171.
[19] C.L. Fu, W.S. Yang, X. Chen, D.G. Evans, Nafion composite film modified electrode, Electrochem. Commun. 11 (2009) 997–1000.
[20] P.V. Kamat, Graphene-based nanoarchitectures. anchoring semiconductor and metal nanoparticles on a two-dimensional carbon support, J. Phys. Chem. Lett. 1 (2010) 520–527.
[21] S.J. Guo, D. Wen, Y. Zhai, S.J. Dong, E.K. Wang, Platinum nanoparticle ensemble-on-graphene hybrid nanosheet: a new electrode material for electrochemical sensing, ACS Nano 4 (2010) 3959–3968.
[22] K.J. Huang, J. Li, Y.M. Liu, X.Y. Cao, S. Yu, M. Yu, electrode functionalized with gold nanoparticles and a Nafion-cysteine conjugate, Microchim. Acta 177 (2012) 419–426.
[23] Y. Luo, H. Liu, Q. Rui, Y. Tian, Detection of extracellular H_2O_2 released from human liver cancer cells based on TiO_2 nanoneedles with enhanced electron transfer of cytochrome *c*, Anal. Chem. 81 (2009) 3035–3041.
[24] L.C. Jiang, W.D. Zhang, Electrodeposition of TiO_2 nanoparticles on multiwalled carbon nanotube arrays for hydrogen peroxide sensing, Electroanal. 21 (2009) 988–993.
[25] D. Chen, L. Tang, J. Li, Graphene-based materials in electrochemistry, Chem. Soc. Rev. 39 (2010) 3157–3180.
[26] M. Pumera, Graphene-based nanomaterials and their electrochemistry, Chem. Soc. Rev. 39 (2010) 4146–4157.
[27] Y. Fan, H.T. Lu, J.H. Liu, C.P. Yang, Q.S. Jing, Y.X. Zhang, X.K. Yang, K.J. Huang, Hydrothermal preparation and electrochemical sensing properties of TiO_2–graphene nanocomposite, Colloids Surf. B: Biointerfaces 83 (2011) 78–82.
[28] Z.M. Liu, Y. Yang, H. Wang, Y.L. Liu, G.L. Shen, R.Q. Yu, A hydrogen peroxide biosensor based on nano-Au/PAMAM dendrimer/cystamine modified gold electrode, Sensors Actuators B 106 (2005) 394–400.
[29] Y. Xiao, F. Patolsky, E. Katz, J.F. Hainfeld, I. Willner, "Plugging into enzymes" nanowiring of redox enzymes by a gold nanoparticle, Science 299 (2003) 1877–1881.
[30] G. Frens, Controlled nucleation for the regulation of the particle size in monodisperse gold suspensions, Nat. Phys. Sci. 241 (1973) 20–22.
[31] W.S. Hummers, R.E. Offeman, RE preparation of graphitic oxide, J. Am. Chem. Soc. 80 (1958) 1339–1340.
[32] N.I. Kovtyukhova, P.J. Ollivier, B.R. Martin, T.E. Mallouk, S.A. Chizhik, E.V. Buzaneva, A.D. Gorchinskiy, Layer-by-layer assembly of ultrathin composite films from micron-sized graphite oxide sheets and polycations, Chem. Mater. 11 (1999) 771–778.
[33] H. Chen, J.H. Jiang, Y. Huang, T. Deng, J.S. Li, G.L. Shen, R.Q. Yu, An electrochemical impedance immunosensor with signal amplification based on Au-colloid labeled antibody complex, Sensors Actuators B 117 (2006) 211–218.
[34] J.H. Lin, C.Y. He, L.J. Zhang, S.S. Zhang, Sensitive amperometric immunosensor for [alpha]-fetoprotein based on carbon nanotube/gold nanoparticle doped chitosan film, Anal. Biochem. 384 (2009) 130–135.
[35] X.Q. Ran, R. Yuan, Y.Q. Chai, C.L. Hong, X.Q. Qian, A sensitive amperometric immunosensor for alpha-fetoprotein based on carbon nanotube/DNA/Thi/nano-Au modified glassy carbon electrode, Colloids Surf. B: Biointerfaces 79 (2010) 421–426.
[36] M. Giannetto, L. Elviri, M. Careri, A. Mangia, G. Mori, A voltammetric immunosensor based on nanobiocomposite materials for the determination of alpha-fetoprotein in serum, Biosens. Bioelectron. 26 (2011) 2232–2236.
[37] H.L. Su, R. Yuan, Y.Q. Chai, Y. Zhuo, C.L. Hong, Z.Y. Liu, X. Yang, Multilayer structured amperometric immunosensor built by self-assembly of a redox multi-wall carbon nanotube composite, Electrochim. Acta 54 (2009) 4149–4154.
[38] W.B. Liang, W.J. Yi, S.H. Li, R. Yuan, A. Chen, S. Chen, G.M. Xiang, C.M. Hu, A novel, label-free immunosensor for the detection of α-fetoprotein using functionalised gold nanoparticles, Clin. Biochem. 42 (2009) 1524–1530.
[39] Y. Li, W.B. Liang, L.C. Fang, H. Huang, J. Deng, J.S. Zheng, Disposable amperometric immunosensor based on layer-by-layer electro-depositing of the nanogold particles, prussian blue-modified indium tin oxide for determination of α-fetoprotein, J. Chem. Sci. 121 (2009) 1069–1076.
[40] Y.X. Liu, R. Yuan, Y.Q. Chai, C.L. Hong, S. Guan, Preparation of a composite film electrochemically deposited with chitosan and gold nanoparticles for the determination of a-1-fetoprotein, Bioprocess Biosyst. Eng. 33 (2010) 613–618.

Ke-Jing Huang received his PhD in 2006 from Wuhan University, and then undertook postdoctoral studies at Nanjing University. Presently, he is an associate professor at Xinyang Normal University. His research interests include electrochemical analysis, chromatography, electrochemical sensors and biosensors.

Jing Li is a graduate student at Xinyang Normal University. Her current researches include graphene-based electrochemical sensors and biosensors.

Ying-Ying Wu is an undergraduate student at Xinyang Normal University. Her current researches include electrochemistry analysis and electrochemical materials.

Yang-Ming Liu received his PhD in 2002 from Wuhan University. Presently, he is a professor at Xinyang Normal University. His research interests include bioelectrochemistry and electrochemical materials.